Arabian Journal of Chemistry (2021) **14**, 102902

King Saud University

Arabian Journal of Chemistry

www.ksu.edu.sa
www.sciencedirect.com

ORIGINAL ARTICLE

Treatment of iron ore beneficiation plant process water by electrocoagulation

Daisy Das, Barun Kumar Nandi *

Department of Fuel Minerals and Metallurgical Engineering, Indian Institute of Technology (Indian School of Mines), Dhanbad, Dhanbad 826004, Jharkhand, India

Received 19 August 2020; accepted 1 November 2020
Available online 10 November 2020

KEYWORDS

Electrocoagulation;
Process water;
Wastewater treatment;
Metal ion removal;
Mineral processing

Abstract Process water collected from the iron ore beneficiation plant was treated by electrocoagulation (EC) process to make it suitable for reuse or safe for discharge. Experimental studies were carried out towards efficient removal of the various metal ions such as iron (Fe), chromium (Cr), copper (Cu), zinc (Zn), manganese (Mn), lead (Pb), aluminum (Al) from process water along with monitoring of total dissolved solids (TDS), turbidity, conductivity, salinity. The influence of various operating parameters of EC, such as electrode material, electrode configuration, current density, inter-electrode distance, and solution conductivity, were explored for effective treatment of process water. Experimental results showed that aluminum electrodes at monopolar mode with a current density of 68.50 A/m^2, an inter-electrode distance of 1 cm, and solution conductivity of 1033 μS/cm were the ideal operating conditions to get treated water with a removal efficiency of 99.95%, 99.46%, 99.33%, 97.99%, 73.44% for Fe, Cr, Pb, Mn, and Cu ions respectively after 60 min of EC with electric energy consumption of 3.93 kWh/m^3 and operating cost of 0.6115 US$/m^3. X Ray Diffraction analysis of EC generated sludge confirmed the exclusion of major elements like Fe, Cr, Cu, Zn, Mn, Pb, Al as well as trace elements such as Nickel, Cobalt, Magnesium, Titanium, Vanadium, Zinc, Neodymium, Samarium, Yttrium, etc. from process water.

1. Introduction

Release and transport of metal ions from active mines and mineral beneficiation plants to the environment pose a threat to different water bodies. Water originated from mineral processing units contains different types of metal ions, organic compounds, total dissolved solids (TDS), etc. as major pollutants (Brooks et al., 2019). Post beneficiation process, such wastewater known as process water is either recycled or stored in tailings ponds after primary treatment (Wu et al., 2019). During the longer duration of storage in tailing ponds, contaminated water percolates through the soil and eventually reaches the groundwater (Brooks et al., 2019). During heavy rain, some of the water overflows the tailing ponds and enters various surface water bodies like ponds, rivers, canals, etc. Release of such metal ion-contaminated water in the surround-

* Corresponding author.
E-mail address: barun@iitism.ac.in (B.K. Nandi).
Peer review under responsibility of King Saud University.

ELSEVIER Production and hosting by Elsevier

https://doi.org/10.1016/j.arabjc.2020.11.008
1878-5352

ing environment seriously affects agriculture and hazardous for human health due to its consumption through the food chain. In many cases, mineral processing plants face difficulty to get massive amounts of freshwater for plant operation. However, if process water is treated suitably to remove various metal ions and treated water is recycled to plant, quantity of freshwater consumption may be reduced.

Substantial numbers of research work have been reported in the literature on the effect of mine waters, particularly acid mine water to nearby water bodies affecting the water quality and their remediation (Arefieva et al., 2019; Naidu et al., 2019; Qina et al., 2019) Suitable treatment techniques for the treatment of acid mine water also have been reported by many authors using adsorption, electrocoagulation, membrane separation, etc. (Silva et al., 2012; Nariyan et al., 2017). Most of the research work has conveyed that the treatment of such water is possible even on at large scale. However, very little attention has been given on treatment and recycling of mineral beneficiation plant process water. Many researchers proposed conventional techniques like flocculation- coagulation, fenton process and chemical flocculation along with the adsorption process to remove metal ions from contaminated water (Shahedi et al., 2020; Elnakar and Buchanan, 2020). For large-scale application, adsorption techniques have limitations in terms of selectivity of pollutants and their adsorption capacity. Except for activated carbon, clay-based adsorbents are highly selective for any particular metal ion or organic contaminants. In this context, electrocoagulation (EC) based separation can be applied for all types of pollutants, including metal ions, organic pollutants, TDS, turbidity, etc. In recent years EC has been evolved as a promising method for water treatment for various researchers (Govindan et al., 2020; Silva et al., 2018). During EC process, in situ production of insoluble metal hydroxide flocs such as ($Al(OH)_{3(S)}$ or $Fe(OH)_{3(S)}$) occur depending upon the anode material (Al or Fe). Summary of such electrochemical reactions (for Fe and Al anode) are summarized below (Canizares et al., 2007):

$$\text{For Fe electrodes}: \quad 4Fe_{(s)} \rightarrow 4Fe^{2+}_{(aq)} + 8e^- \tag{1}$$

$$2H_2O \rightarrow O_{2(g)} + 2H_{2(g)} \tag{2}$$

$$4Fe^{2+}_{(aq)} + 10H_2O_{(l)} + O_{2(g)} \rightarrow 4Fe(OH)_{3(s)} + 8H^+_{(aq)} \tag{3}$$

$$8H^+_{(aq)} + 8e^- \rightarrow 4H_{2(g)} \tag{4}$$

$$\text{For Al electrodes}: \quad Al \rightarrow Al^{3+}(aq) + 3e^- \tag{5}$$

$$2H_2O \rightarrow O_{2(g)} + 2H_{2(g)} \tag{6}$$

$$Al^{3+}(aq) + 3H_2O \rightarrow Al(OH)_{3(S)} + 3H^+(aq) \tag{7}$$

$$3H^+_{(aq)} + 3e^- \rightarrow 1.5H_{2(g)} \tag{8}$$

These freshly generated metal hydroxide complexes ($Al(OH)_{3(S)}$ or $Fe(OH)_{3(S)}$) have the high surface area and high ionic characteristics. Presence of freshly generated various active ionic species helps in ionizing the other organic and inorganic species present in water and form water-insoluble materials. As a result, freshly generated metal hydroxide complexes ($Al(OH)_{3(S)}$ or $Fe(OH)_{3(S)}$) easily trap different types of ionic pollutants such as ions of Fe, Cr, Pb, Mn, etc. present in water and eventually separated them as water-insoluble sludge after undergoing coagulation adsorption, flocculation, and co-precipitation (Das and Nandi, 2020). EC process bears several advantages like minimum expenditure, easier installation, low chemical consumption, more cost-effective and lesser treatment time. Also, EC produces very less amount of sludge as compared to other coagulation techniques, readily settleable and easy to dewater (Hashim et al., 2017). Although some work has been reported on the treatment of acid mine drainage and metal ion rich mine wastewater using conventional process, almost no research work has been reported on iron ore beneficiation plant process water. As a result, most of the iron ore beneficiation plant faces difficulty in discharging large volumes of water as well as a shortage of fresh water to operate the plant. Hence, suitable treatment technologies needs to be explored to operate iron ore beneficiation plant in environment-friendly manner.

The present work aims to verify the applicability of EC process towards the treatment of mineral beneficiation unit process water. Iron ore process water obtained from the beneficiation plant was treated using EC process. Impact of various operating conditions like most effective pair of the electrode, electrode configuration, current density (j), inter-electrode distance (i_d), and solution conductivity (S) on metal ions removal as well as various water quality parameters such as TDS, conductivity, salinity have been assessed. Kinetic analysis of EC has been carried out towards deeper analysis of the effect of current density on metal ion removal. Overall, the present study is expected to improve the water management system in different mineral processing industries and consequently contribute in reducing the contamination of groundwater as well as surface water due to discharge of such pollutant rich water in the nearby areas.

2. Materials and methods

About 100 L of iron ore beneficiation plant process water was collected from iron ore beneficiation plant located in Odisha state, India. After collection, water was brought to the laboratory and kept in a tank for two days to allow suspended particles to settle down. Further, water was filtered using Whatman 1 filter paper (pore size: 11 μm) to remove any suspended solids. EC experiments were conducted using a 2 L beaker considering 1 L of water for 60 min. The schematic of the experimental setup is shown in Fig. 1a. Aluminum (Al, 99% purity) and Iron (Fe, 99% purity) plates with 99% purity and a submerged area of 0.0146 m^2 (length: 0.073 m; width: 0.1 m, thickness: 0.001 m) were used as electrodes. Three different electrode configurations, namely monopolar (M) using two electrodes, series monopolar (SM) using four electrodes and series bipolar (SB) using four electrodes as shown in Fig. 1a–c respectively, have been used. All the experiments were conducted at room temperature (25 ± 2 °C) and the natural pH (pH: 7.09) of the water. Magnetic stirrer (Model: SPINIT Digital MC-02, TARSON) operating at 200 RPM was used for uniform mixing of water and flocs during EC. DC power source (Model: L6410S, APLAB) was used for providing the desired electricity. Sodium chloride (NaCl) salt was added to enhance the conductivity of the water. Table 1 presents the various range of operating conditions considered in the study. About 3–5 ml of water sample was col-

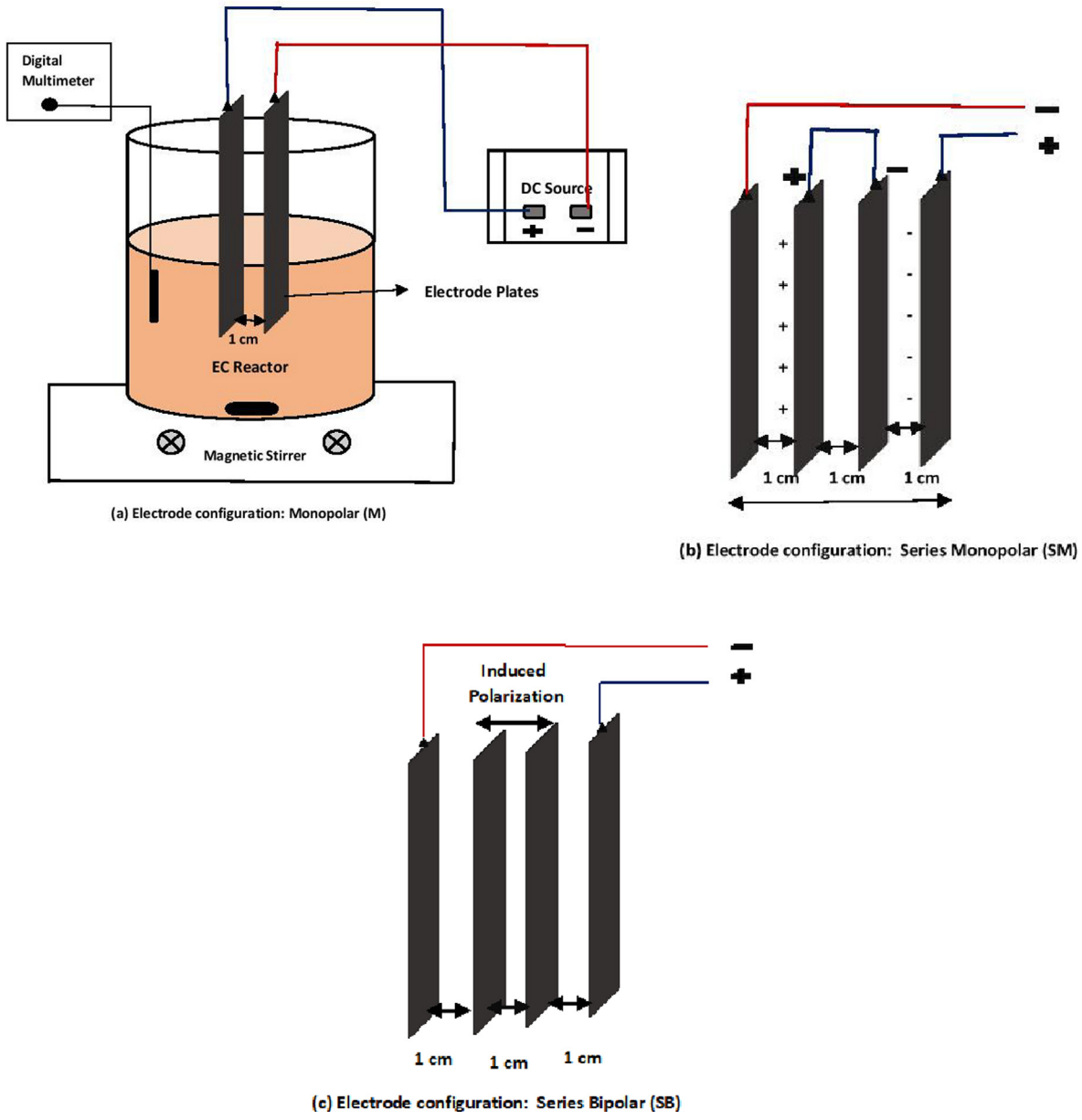

Fig. 1 Schematic diagram of the experimental set-up with (a) Monopolar (M) electrode configuration, (b) Series monopolar (SM) electrode configuration and (c) Series bipolar (SB) electrode configuration.

lected at an interval of 10 min and filtered using filter paper and used for further analysis. After every experiment, the electrode surface were cleaned using abrasive paper and followed by diluted hydrochloric acid and water wash to remove all the impurities. Untreated and treated water sample was analyzed for the presence of different metal ions (Cr, Fe, Mg, Zn, Cu, Pb and Al) using Atomic Absorption Spectrometer (Model: iCE 3000 Series, Thermo scientific) after calibrating with a standard solution for each metal ion (Das and Nandi, 2020). TDS, salinity, conductivity, and pH of the untreated water and treated water were measured using a digital multimeter (Model: PC2700, EUTECH) (Das and Nandi, 2019a). Turbidity was estimated using a turbidity meter (Model: TN-100, Thermo Scientific) (Das and Nandi, 2020). For the characterization of the generated sludge, XRD analysis was conducted using the XRD analyzer available at CIMFR, Dhanbad. In the present work all the experiments were performed thrice and $\pm 0.50\%$ variations of individual values were observed. The removal efficiency of each metal ion is calculated using the following equation:

$$Removal\ \% = \frac{S_o - S}{S_o} \times 100 \tag{9}$$

where S_o and S are the initial and residual concentration of metal ions at any time.

Electric energy consumption (EEC) per unit volume (KWh/m^3) for various operating condition was estimated by the following Eq. (10) (Das and Nandi, 2019b):

Table 1 Range of operating parameters considered for EC experiments.

Effect of operating conditions studied	Range considered	Conditions kept constant
Electrode material (Anode/Cathode)	Al/Al, Fe/Fe, Al/Fe, Fe/Al	Mode: M, j-68.50 A/ m^2, i_d-1 cm, S-1033 μS/cm
Electrode configuration mode	M, SM, SB	Electrode: Al/Al, j-68.50 A/ m^2, i_d-1 cm, S-1033 μS/cm
Current density (j, A m^{-2})	34.25, 51.37, 68.50, 86.20 A/ m^2	Mode: M, Electrode: Al/Al, i_d-1 cm, S- 1033 μS/cm
Inter-electrode distance, (i_d, cm)	1.0, 1.5, 2.0 cm	Mode: M, Electrode: Al/Al, j-68.50 A/m^2, S-1033 μS/cm
Solution conductivity (S, μS cm^{-1})	1033, 1454, 1888 μS/cm NaCl: 0.5, 0.75, 1.0 g/L	Mode: M, Electrode: Al/Al, j-68.50 A/m^2, i_d-1 cm

Table 2 Summary of major metal ions present in process water along with other parameters.

Sl. No	Parameters	Values	Permissible limit (WHO, 2004)
1	Fe (mg/L)	115.24	0.30
2	Cr (mg/L)	7.10	0.05
3	Cu (mg/L)	0.27	1.3
4	Pb (mg/L)	2.68	0.01
5	Mn (mg/L)	0.96	0.05
6	Al (mg/L)	24.75	5
7	Silica (mg/L	1.29	5–25
8	TDS (mg/L)	130.6	500–700
9	TSS (mg/L)	43,693	25
10	Turbidity (NTU)	977	< 1
11	Conductivity (μS/cm)	178.3	200–2000
12	Resistivity (KΩ)	4.566	–
13	Salinity (mg/L)	95.36	–
14	pH	7.09	6.5–8.5

$$EEC = \frac{(\text{cell voltage, V}) \times \text{applied current, amp}) \times (\text{EC time, hr})}{(\text{water volume, m}^3)} \quad (10)$$

To justify the application of EC process economic evaluation of the present study was estimated by considering the cost of energy consumed and electrode material as these are the major components of operating cost for lab scale units as (Al-Qodah and Al-shannag, 2017):

$$\text{Operating cost } (\text{US}/\text{m}^3) = \left[a \cdot C_{energy} + b \cdot C_{electrode}\right] \quad (11)$$

where a (0.083 US$/kWh) and b (2.046 US$/kg Al) are the cost of electricity per unit and iron per kg respectively considered as per Indian market price in 2018 (Das and Nandi, 2020).

$$C_{energy} = \frac{Cell\ \ voltage\ \ (V) \times current\ \ (A) \times time\ \ (s)}{sample\ \ volume\ \ (m^3)} \quad (12)$$

$$C_{electrode} = \frac{applied\ \ current\ \ (A) \times EC\ \ time\ \ (s) \times molecular\ \ mass\ \ of\ \ Al\ \ \left(\frac{g}{mol}\right)}{eletrone\ \ transfered \times Faraday's\ \ constant \times Volume\ \ (m^3)} \quad (13)$$

3. Results and discussions

3.1. Characterization of water before treatment

Table 2 shows the concentrations of various metal ions and other water quality parameters present in process water collected from iron ore beneficiation plant followed by settling and filtration. It is observed from the results that the concentration of total Fe, Cr, Pb, Mn and turbidity are found to be 115.24 mg/L, 7.10 mg/L, 2.68 mg/L, 0.96 mg/L and 977 NTU respectively. Overall, values of Cu and Al ions, TDS, conductivity, pH, etc. were found to be within world health organization (WHO) permissible limit. As the concentration of Fe, Cr, Pb and Mn were above the permissible limit, removal of Fe, Cr, Pb and Mn were analyzed in-detailed in the present study.

3.2. Effect of anode and cathode material:

To evaluate the effect of electrode material on metal ions removal, different combination on anode and cathode material were used. Fig. 2a-d shows the removal efficiency of Fe, Cr, Pb and Mn at various electrode combinations after 60 min of EC. From all the figures, it can be observed that Al/Al combinations give better removal for Fe, Pb and Mn ions and Fe/Fe combination gives better Cr ions removal. From Fig. 2a it is observed that the removal efficiency of Fe after 60 min EC was 99.95% for Al/Al electrode combination compared to 98.34%, 99.29% and 99.92% for Fe/Fe, Al/Fe and Fe/Al electrode combinations, respectively. From Fig. 1b it is observed that removal efficiency of Cr ions after 60 min of EC were 99.46%, 99.68%, 99.42% and 99.54% for Al/Al, Fe/Fe, Al/Fe and Fe/Al, respectively. Removal efficiency of Pb ions after 60 min of EC were 99.33%, 96.92%, 98.13% and 97.48% for Al/Al, Fe/Fe, Al/Fe and Fe/Al, respectively (Fig. 2c). For Mn ions removal efficiency were 97.99%, 93.54%, 95.61% and 90.37% Al/Al, Fe/Fe, Al/Fe and Fe/Al, respectively (Fig. 2d). Higher Cr ions removal for Fe/Fe combinations was due to faster reduction of total chromium ions to trivalent chromium ions in the presence of $Fe(OH)_3$ flocs (Lu et al., 2016). Overall, better performance of Al/Al electrode combinations over Fe/Fe and other electrode combinations was due to higher electro dissolution of the aluminum anode at the same electric voltage applied and generation of more coagulants, which enhances Fe, Cr, Pb and Mn ions removal. In other words, Al possesses higher electrode oxidation potential ($E^\circ = -1.66$ V) in the electrochemical series of elements compared to Fe ($E^\circ = +0.44$ V), it loses electrons easily compared to Fe which makes the coagulation, adsorption and precipitation process faster (Das and Nandi, 2019a). Table 3 shows the final values of TDS, turbidity, conductivity, salinity, Al ions and Cu ions after 60 min of EC treatment for various combinations of electrodes. It is seen that for Al/Al combination, all the values are lower than other combinations, but all the values are found within the permissible limit (Table 2). Since Al/Al electrode combination shows higher removal efficiency

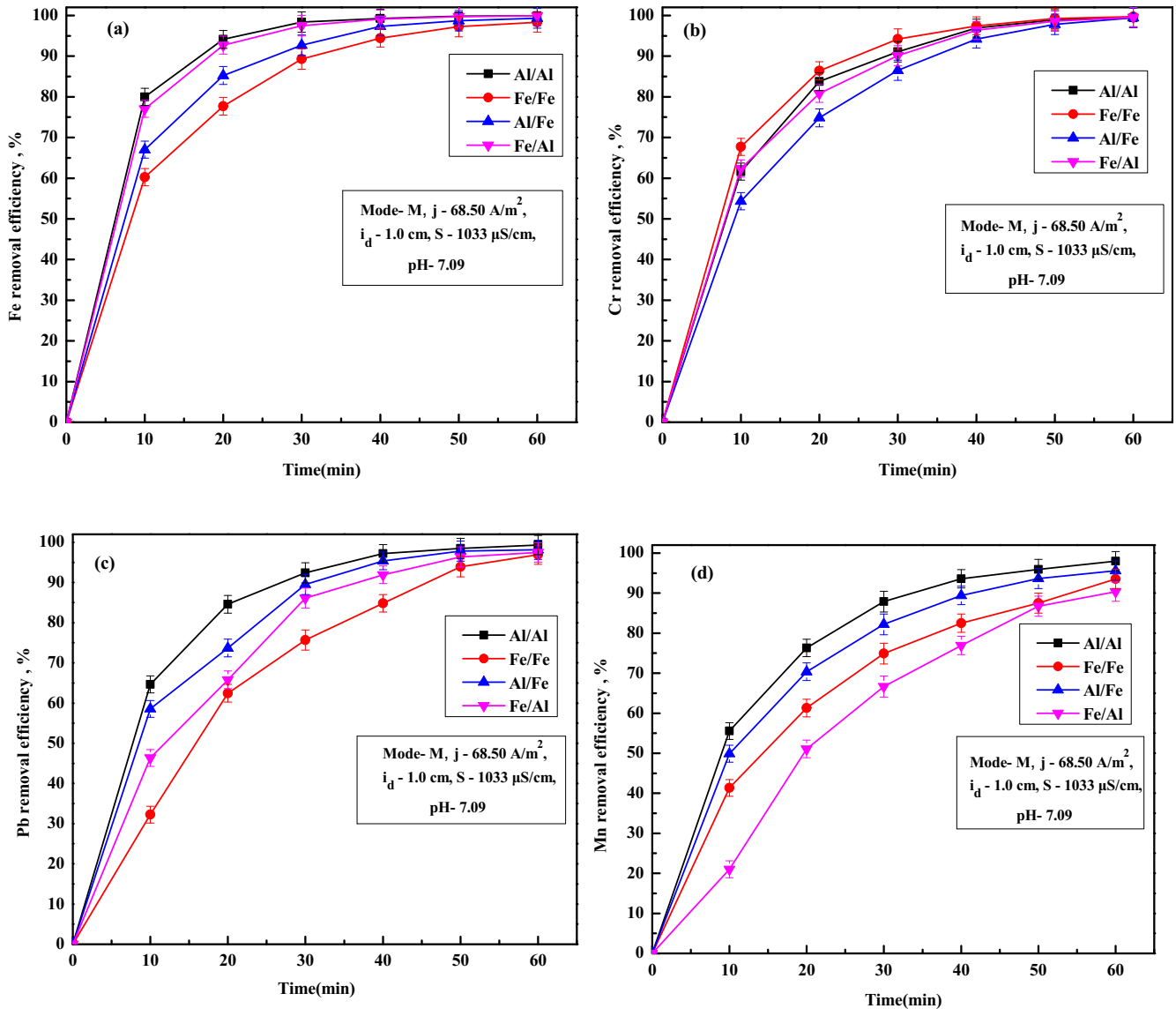

Fig. 2 Effect of different metal combinations as anode/cathode on removal of (a) Fe, (b) Cr, (c) Pb and (d) Mn ions.

Table 3 Values of TDS, turbidity, salinity, conductivity, Al ions and Cu ions at various anode and cathode material after 60 min of EC for different meal combinations as anode/cathode.

Electrode material	TDS (mg/L)	Turbidity (NTU)	Salinity (mg/L)	Conductivity (µS/cm)	Al ions (mg/L)	Cu ions (mg/L)	EEC (kWh/m^3)
Al/Al	85.45	0.89	92.61	522	0.72	0.07	3.93
Fe/Fe	106.21	0.94	98.21	574	1.27	0.005	4.66
Al/Fe	102.35	0.92	101.5	571	1.67	0.03	4.33
Fe/Al	110.41	0.98	105.3	612	1.43	0.008	4.06

for Fe ions with highest initial concentration of 115.24 mg/L and adequate removal efficiency for Cr, Pb and Mn ions also, Al/Al pair of the electrode was used for further experiments.

3.3. Effect of electrode configuration

Fig. 3a–d shows the variations of residual ion concentration of Fe, Cr, Pb and Mn ions with M, SM and SB electrode configuration using Al/Al electrodes. From Fig. 3a–d, it is observed that, SB electrode configuration gives faster ion removal compared to M and SM. Removal efficiency of Fe ion were 99.95%, 99.98%, and 99.98% for M, SM and SB after 60 min of EC. For Cr ions removal efficiency were 99.46%, 99.63% and 99.84% for M, SM and SB (Fig. 3b). Similarly, for Pb ions removal efficiency were 99.33%, 99.70% and 99.83% (Fig. 3c), for Mn ions removal efficiencies were

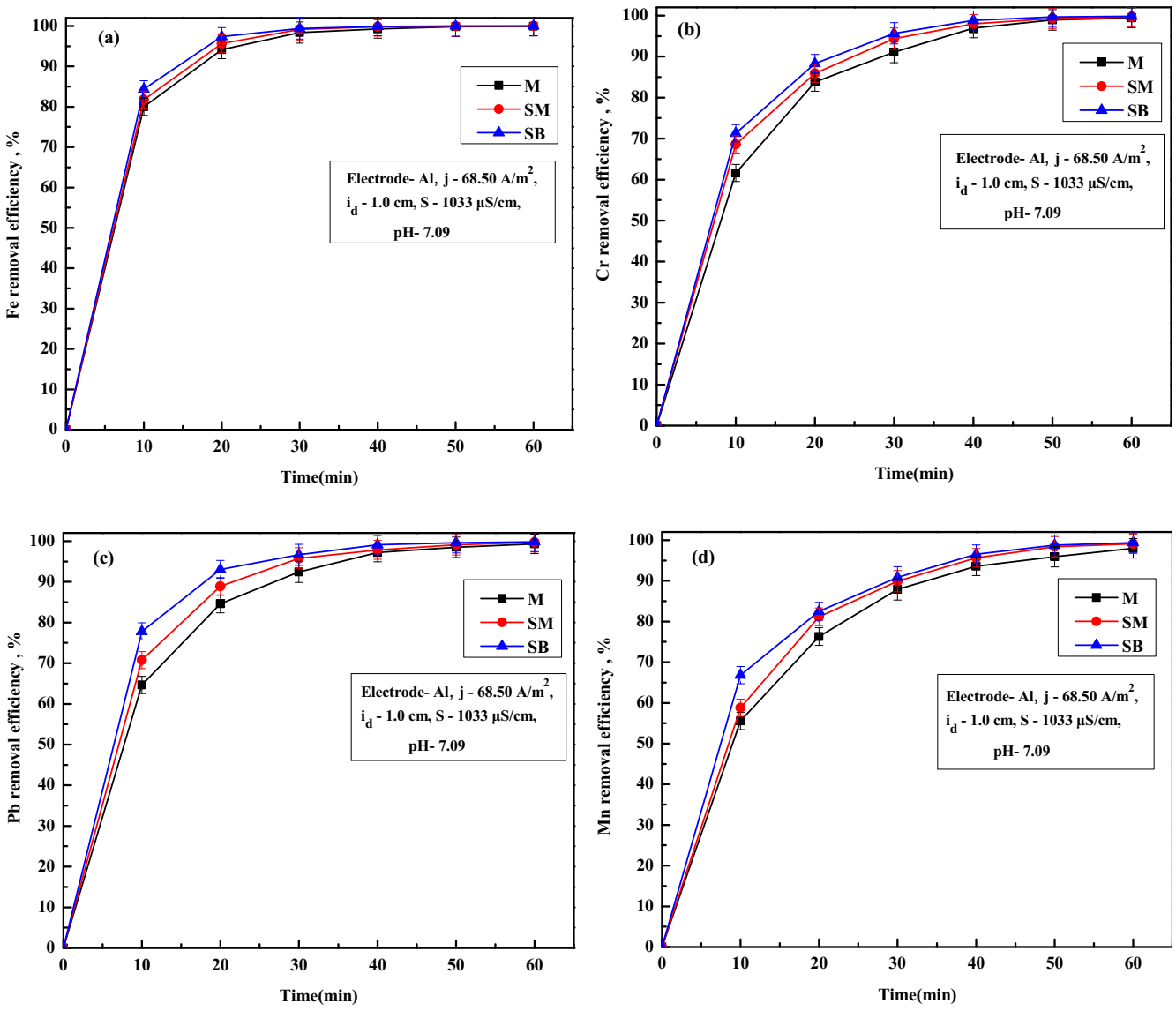

Fig. 3 Effect of different electrode configuration on removal of (a) Fe, (b) Cr, (c) Pb and (d) Mn ions.

97.99%, 99.12% and 99.35% (Fig. 3d) for M, SM and SB, respectively. Better ion removal efficiency for SM and SB mode was due to availability of higher electrode surface area and eventually better flocs generation. Better ion removal from SB mode compared to SM mode was due to higher electro dissolution of the anodes at bipolar mode (Modirshahla et al., 2008). Table 4 infers that the final value of TDS (103.27 mg/L) and turbidity (1.24 NTU) are slightly higher for SB mode compared to M mode. Higher values of TDS and turbidity for SM and SB mode were due to the presence of excessive flocs, which acts as a secondary pollutant to the water. Thus, the results show that all the values of final TDS, turbidity, conductivity, salinity, Al ions and Cu ions, were found within the permissible limit for all the modes. EEC for M, SM and SB was found to be 3.93, 7.47 and 11 kWh/m^3 with corresponding electrode potential of 11.8, 22.4 and 33 V, respectively. Such observations inferred that EEC increases with increase in number of electrode plates due to increase in necessary electrode potential. The operating cost at electrode configuration of M, SM and SB are estimated as 0.6115, 0.9429 and 1.2733 US$/$m^3$ respectively. To keep TDS, turbidity and salinity values on the lower side and considering the complexity of using more than two electrodes, further experiments were conducted using M mode, which also give satisfactory removal of Fe, Cr, Pb and Mn ions.

3.4. Effect of current density

Current density is an influential operating condition in EC as it controls flocs generation rate and pollutant removal rate. Fig. 4a-d shows the variations of removal efficiencies of Fe, Cr, Pb and Mn ion in treated water for various current densities. From Fig. 4a, it is observed that the removal efficiency Fe ion increases from 99.69% to 99.97% as CD increases from 34.25 to 86.20 A/m^2. Similar results were also observed for Cr, Pb and Mn ions (Fig. 4b–d). For all the ions, permissible limits were attained at almost 40 min for higher CD of 68.50 A/ m^2 and above. Removal efficiency were 95.44%, 96.50%,

Table 4 Values of TDS, turbidity, salinity, conductivity, Al ions and Cu ions for different electrode configuration using Al electrode.

Electrode configuration	TDS (mg/L)	Turbidity (NTU)	Salinity (mg/L)	Conductivity (μS/cm)	Al ions (mg/L)	Cu ions (mg/L)	EEC (kWh/m^3)	OC (US$/m^3)
M	85.45	0.89	92.61	522	0.72	0.07	3.93	0.6115
SM	92.42	0.97	93.34	501	0.79	0.02	7.47	0.9429
SB	103.27	1.24	94.35	478	0.69	0.01	11	1.2733

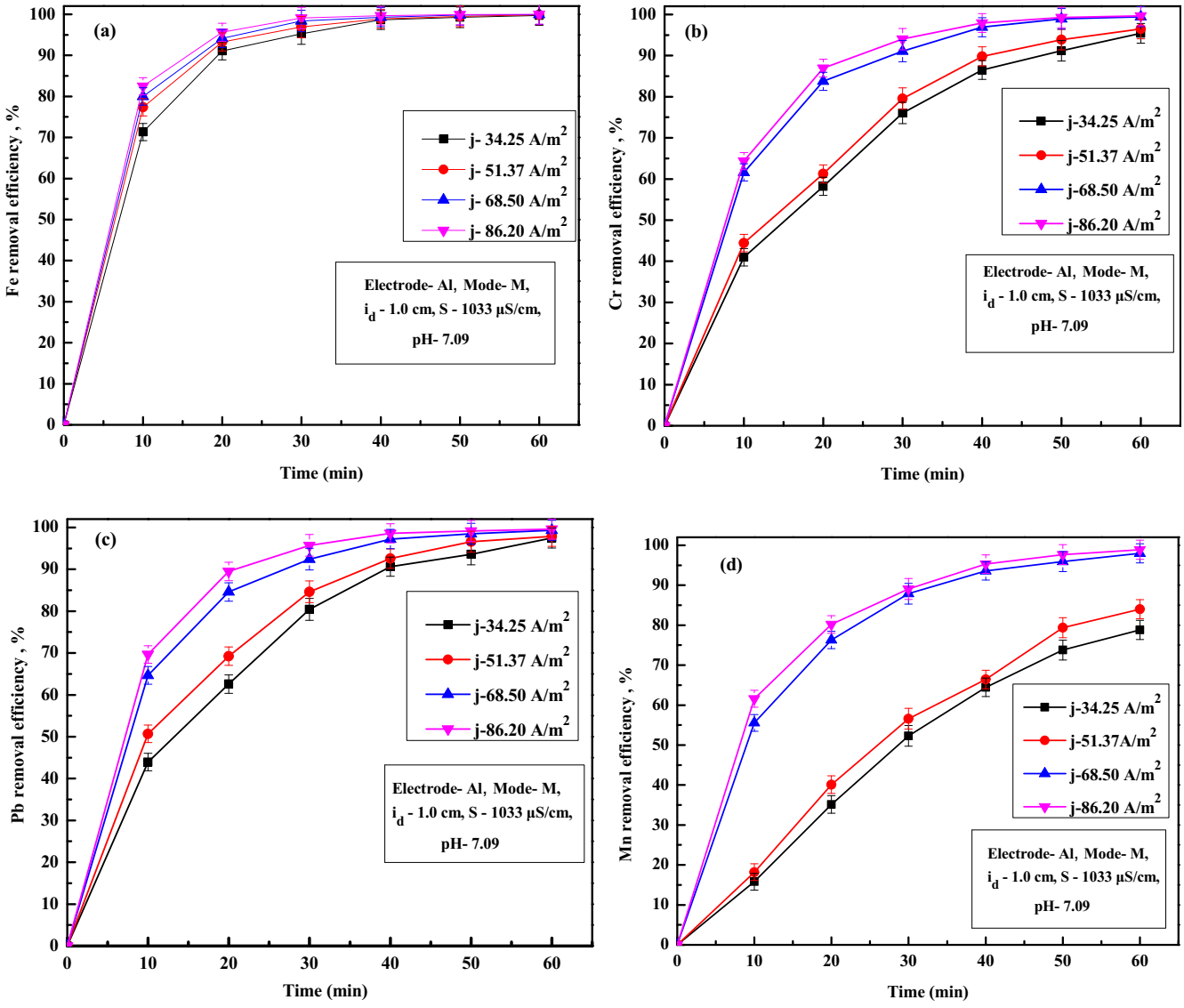

Fig. 4 Effect of current densities on removal of (a) Fe, (b) Cr, (c) Pb and (d) Mn ions.

99.46% and 99.65% for Cr ions, 97.48%, 97.86%, 99.33% and 99.61% for Pb ions and 78.82%, 83.99%, 97.99% and 98.87% for Mn ions for CD of 34.25, 51.37, 68.50 and 86.20 A/m^2, respectively after 60 min of EC. An increase in metal ions removal with current density were attributed to the increase of in situ coagulant production with larger size and surface area due to faster dissolution of the anode, which results in rapid pollutant ions removal (Akbal and Camcı, 2011). Variations in removal efficiency of Al and Cu ions for various current densities are shown in Fig. 6a and b. It is observed from Fig. 6a that, removal efficiency of Al ions increases to 98%, within 10 min of EC for current density of 86.20 A/m^2 and then varied slightly during the entire EC duration. Cu ions concentration decreases gradually with EC time. Obtained values of TDS, turbidity, conductivity, salinity, Cu ions, Al ions and final pH after 60 min of EC for different current densities

Table 5 Values of TDS, turbidity, salinity, conductivity, Al ions and Cu ions at various current density after 60 min of EC.

Current density (A/m^2)	TDS (mg/L)	Turbidity (NTU)	Salinity (mg/L)	Conductivity (μS/cm)	Al ions (mg/L)	Cu ions (mg/L)	pH	EEC (kWh/m^3)	OC (US$/$m^3$)
34.25	101.23	10.01	97.14	656	0.41	0.09	7.25	0.13	0.1265
51.37	92.33	5.02	94.25	596	0.65	0.08	7.28	2.45	0.4009
68.50	85.45	0.89	92.61	522	0.72	0.07	7.36	3.93	0.6115
86.20	79.12	0.70	88.24	498	0.75	0.04	7.52	6.28	0.8626

are summarized in Table 5. From Table 5, it can be seen that, final TDS varied from 101.23 to 79.12 mg/L, conductivity decreased from 656 to 498 μS/cm, turbidity reduced from 10.1 to 0.70 NTU, salinity varied from 97.14 to 88.24 mg/L, copper ions decreased from 0.09 mg/L to 0.04 mg/L, Al ions varied from 0.41 to 0.75 mg/L and final pH varied from 7.25 to 7.52 as the current density increases from 34.25 to 86.20 A/m^2. The decrease in TDS, turbidity, conductivity, salinity, Cu ions with an increase in current density was due to the increased adsorption or entrapment of the pollutant materials by the excess coagulant available in solution at higher current density. Minor increase in Al ions at higher current density is due to the presence of surplus amount of aluminum hydroxide flocs unutilized after EC. However, the

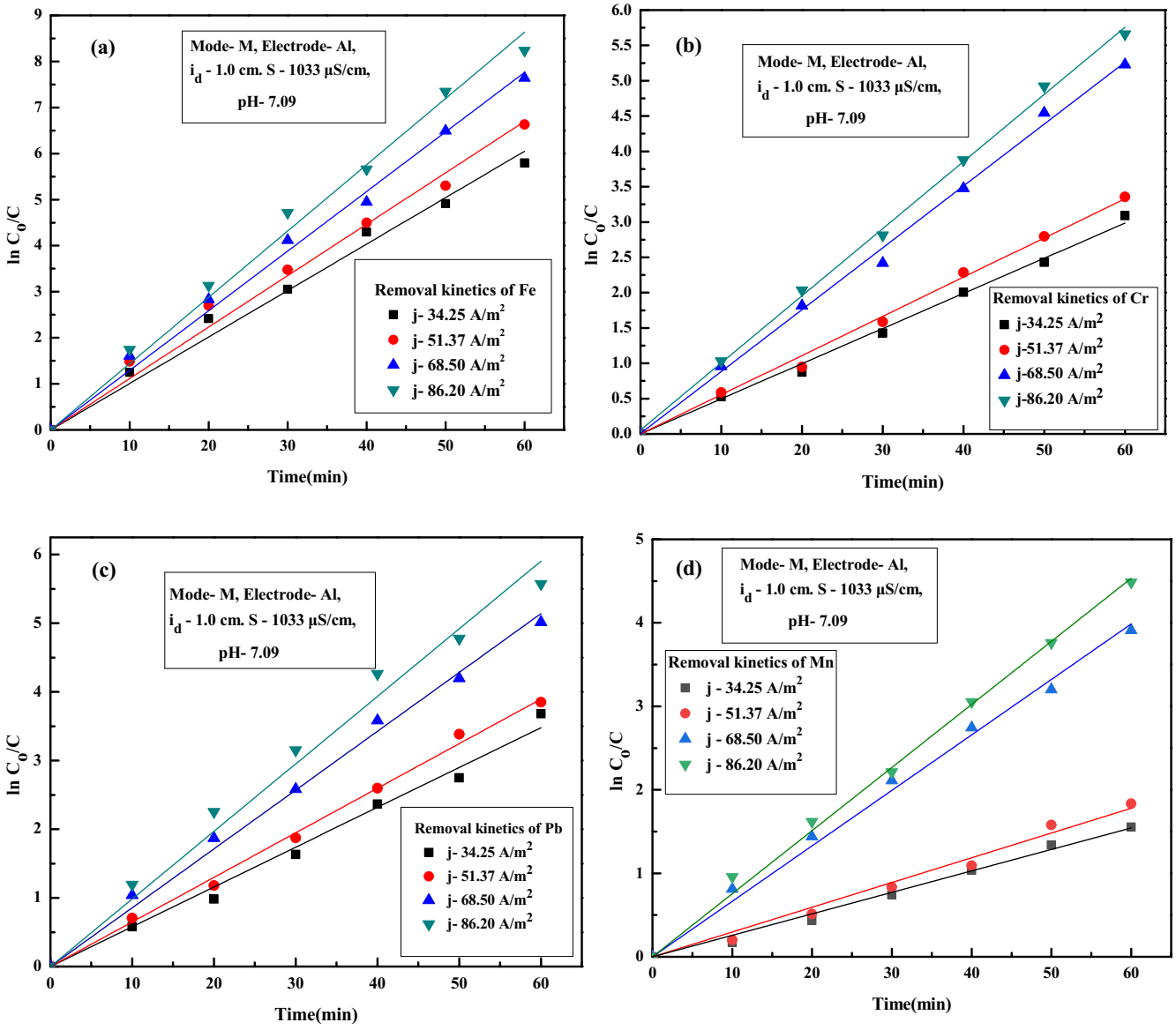

Fig. 5 First-order kinetic model for removal of (a) Fe, (b) Cr, (c) Pb and (d) Mn ions for different current density.

Table 6 Values of rate constant (k) at different current density for Fe, Cr, Pb and Mn ion removal by EC.

Current density (A/m^2)	Rate constant, (k, min^{-1})			
	Fe	Cr	Pb	Mn
34.25	0.1008	0.0497	0.0580	0.0257
51.37	0.1116	0.0555	0.0649	0.0297
68.50	0.1294	0.0877	0.0857	0.0664
86.20	0.1469	0.0936	0.0984	0.0756

presence of excess amounts of Al ions is not desirable as it acts as a secondary pollutant in treated water. The EEC and OC increases from 0.13 to 6.28 kWh/m^3 and 0.1265 to 0.8626 US$/m^3 as CD increases from 34.25 to 86.20 A/m^2. Hence, the use of higher current density needs to be avoided to maintain desirable water quality. Hence, a moderate current density of 68.50 A/m^2 with EEC of 3.93 kWh/m^3 and OC of 0.6115 of US$/m^3 was used for further experiments as desirable removal efficiency up to permissible limit. Such EEC and OC values are lower compared to the EEC and OC reported by Al-Qodah et al. (2020a, 2020b), 2019; Elazzouzi et al. (2019), Dhadge et al. (2018) and many others during treatment of wastewater using hybrid process. Al-Qodah et al. (2020b) reported that combined EC process with granular activated carbon for removal of acid dye at current density of 109.14 A/m^2 gives 20% higher removal efficiency than EC alone but at extremely higher operating cost of 5.033 $/Kg. Elazzouzi et al. (2019) reported that combined EC-floatation process for urban wastewater treatment at optimum condition gives operating cost of 0.80 $/kg and 0.82 $/kg using Al and Fe electrodes. Dhadge et al. (2018) reported that hybrid process of EC and MF gives 98.74%, 95.65%, 93.2% and 100% removal for iron, arsenic, fluoride and microorganisms at current density of 625 A/m^2 and operating cost of 7.91 US$/m^3.

To verify the kinetics of individual metal ions removal, first order kinetic model and second order model were verified. However, it was observed that individual metal ion removal during EC were apparently following first-order kinetic model as follows (Das and Nandi, 2020):

$$\ln\frac{C_o}{C} = kt \tag{14}$$

where C_0 and C specifies the metal ions concentrations of initial and at time t (min) respectively. k denotes the rate constant. Fig. 5a–d shows the first-order model for removal of Fe, Cr, Pb and Mn at different current densities. From all the figures, it is observe that ion removal followed the first-order kinetic model. Obtained values of rate constant k (min^{-1}) for all the metal ions at various current densities are summarized in Table 6. It can be inferred from Table 6 that, with an increase in current density from 34.25 to 86.20 A/m^2, Fe ion removal rate (k) increased from 0.1008 to 0.1469 min^{-1}. Similar trends of results are also observed for removal of Cr ions (k increased from 0.0497 to 0.0936 min^{-1}), Pb ions (k increased from 0.0580 to 0.0984 min^{-1}), and Mn ions (k increased from 0.0257 to 0.0756 min^{-1}). Increase in k with current density was due to the rise in $Al(OH)_3$ flocs generation at higher current density. Due to faster flocs generation rate, the entrapment of ions occurs at a faster speed and thus increases the removal rate.

3.5. Effect of inter-electrode distance

Different inter-electrode distances (i_d) of 1, 1.5 and 2 cm were used to identify the effect of inter-electrode distance on Fe, Cr, Pb and Mn ions removal, and results are shown in Fig. 7a–d. It is observed from Fig. 7a that removal efficiency of Fe ion decreased from 99.95 to 99.85% with an increase in i_d from

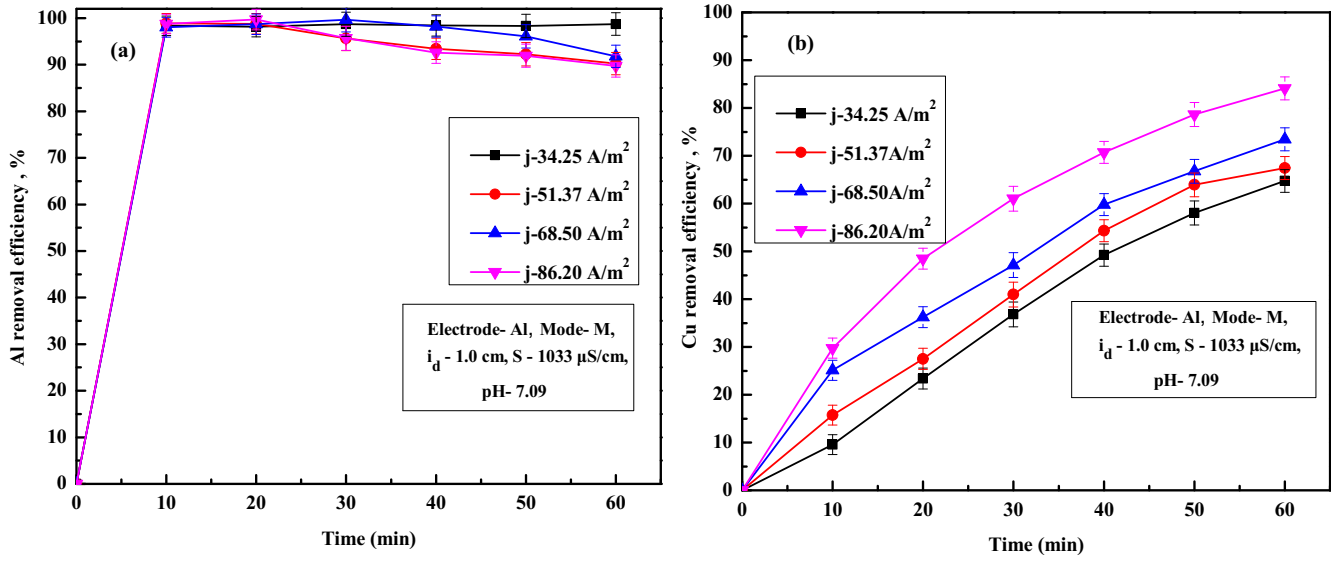

Fig. 6 Variation in removal efficiency at various CD of (a) Aluminum and (b) Copper.

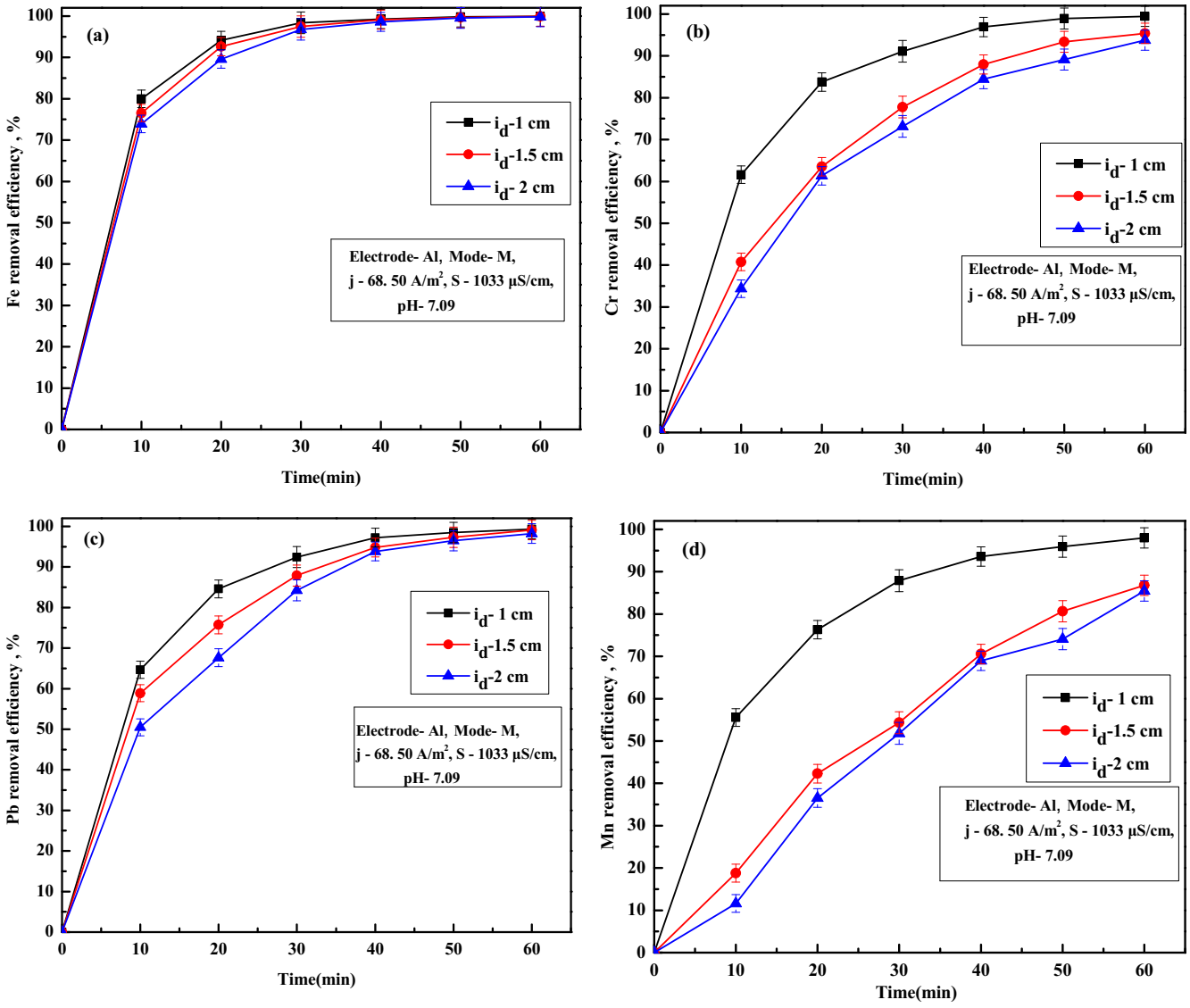

Fig. 7 Effect of different inter-electrode distance on removal of (a) Fe, (b) Cr, (c) Pb and (d) Mn ions.

Table 7 Values of TDS, turbidity, salinity, conductivity, Al ions and Cu ions for different inter-electrode distance after 60 min of EC.

Inter-electrode distance (cm)	TDS (mg/L)	Turbidity (NTU)	Salinity (mg/L)	Conductivity (µS/cm)	Al ions (mg/L)	Cu ions (mg/L)	EEC (kWh/^{3})
1.0	85.45	0.89	92.61	522	0.72	0.07	3.93
1.5	91.28	1.53	96.56	556	0.70	0.08	5.8
2.0	96.47	2.63	102.69	578	0.69	0.10	7.5

1.0 to 2.0 of 60 min of EC. Similar trends of results are also observed for removal of Cr ions (decreased from 99.46% to 93.75%, Fig. 7b), Pb ions (decreased from 99.33% to 98.23%, Fig. 7c), and Mn ions (decreased from 97.99% to 85.44% Fig. 7d). An increase in residual ion concentration with i_d was due to decreases in electrostatic effects of generated flocs. With an increase in i_d, electron transport between the electrodes gets slowed down, flocs generation rate reduced and finally, pollutant ion capture by flocs decreases. Obtained values of TDS, turbidity, conductivity, salinity, Cu ions and Al ions after 60 min of EC for different i_d are summarized in Table 7. From Table 7, it can be observed that final TDS varied from 85.45 to 96.47 mg/L, conductivity varied from 522 to 578 µS/cm, turbidity varied from 0.89 to 2.63 NTU, salinity varied from 92.61 to 102.69 mg/L, copper ions varied from 0.07 to 0.10 mg/L and Al ions varied from 0.7225 to 0.6939 mg/L as i_d increased from 1 to 2 cm. Increase in TDS, turbidity, conductivity, salinity, Cu ions with an increase

in inter-electrode distance was due to reduced electrostatic effects of generated flocs and pollutant materials. Minor decrease in Al ion concentration with an increase in i_d inferred better flocs utilization due to slower EC process. Since higher i_d needs higher voltage to maintain the necessary current density and removal efficiency of most of the ions decreased, a minimal inter-electrode distance of 1 cm was used for all the further experiments.

3.6. Effect of solution conductivity

Since electrical conductivity of process water was low (178.3 µS/cm), some salts need to be added in process water to keep the applied voltage on lower side to maintain necessary current density. In this work, NaCl was added to improve the electrical conductivity of untreated water. For this purpose, experiments were performed with varying NaCl dose of 0.5, 0.75 and 1 g/L to obtain overall conductivity of 1033, 1454 and 1888 µS/cm. Further, experiments were performed with a current density of 68.50 A/m^2 and corresponding Fe, Cr, Pb and Mn removal trends are shown in Fig. 8a–d. It is observed from Fig. 5a–d that overall Fe, Cr, Pb and Mn ion removal efficiency rapidly with an increase in solution conductivity. From Fig. 8a, it is observed that the removal efficiency of Fe ion varied from 99.95 to 99.98% with an increase in conductivity from 1033 to 1888 µS/cm after 60 min of EC. Similar trends of results are also observed for removal of Cr ions (increased from 99.46% to 99.85%), Pb ions (increased from 99.33% to 99.79%), and Mn ions (increased from 97.99% to 99.02%). The permissible limit of all the ions was achieved at lower conductivity at 1033 µS/cm at almost 50 min of EC. The increase in ion removal efficiency with the rise in solution conductivity was due to an increase in ionic activity in solution at higher electrical conductivity, which enhances the pollutant ion removal (Das and Nandi, 2019b). At higher conductivity, higher anodic dissolution occurs, which increases flocs generation rate and ion removal becomes faster. Obtained values of TDS, turbidity, conductivity, salinity, Cu ions and Al ions after 60 min of EC for different conductivity are summarized in Table 8. From this table, it can be observed that final TDS decreased from 85.45 to 72 mg/L, turbidity decreased from 0.89 to 0.79 NTU, copper ions increased from 0.07 to

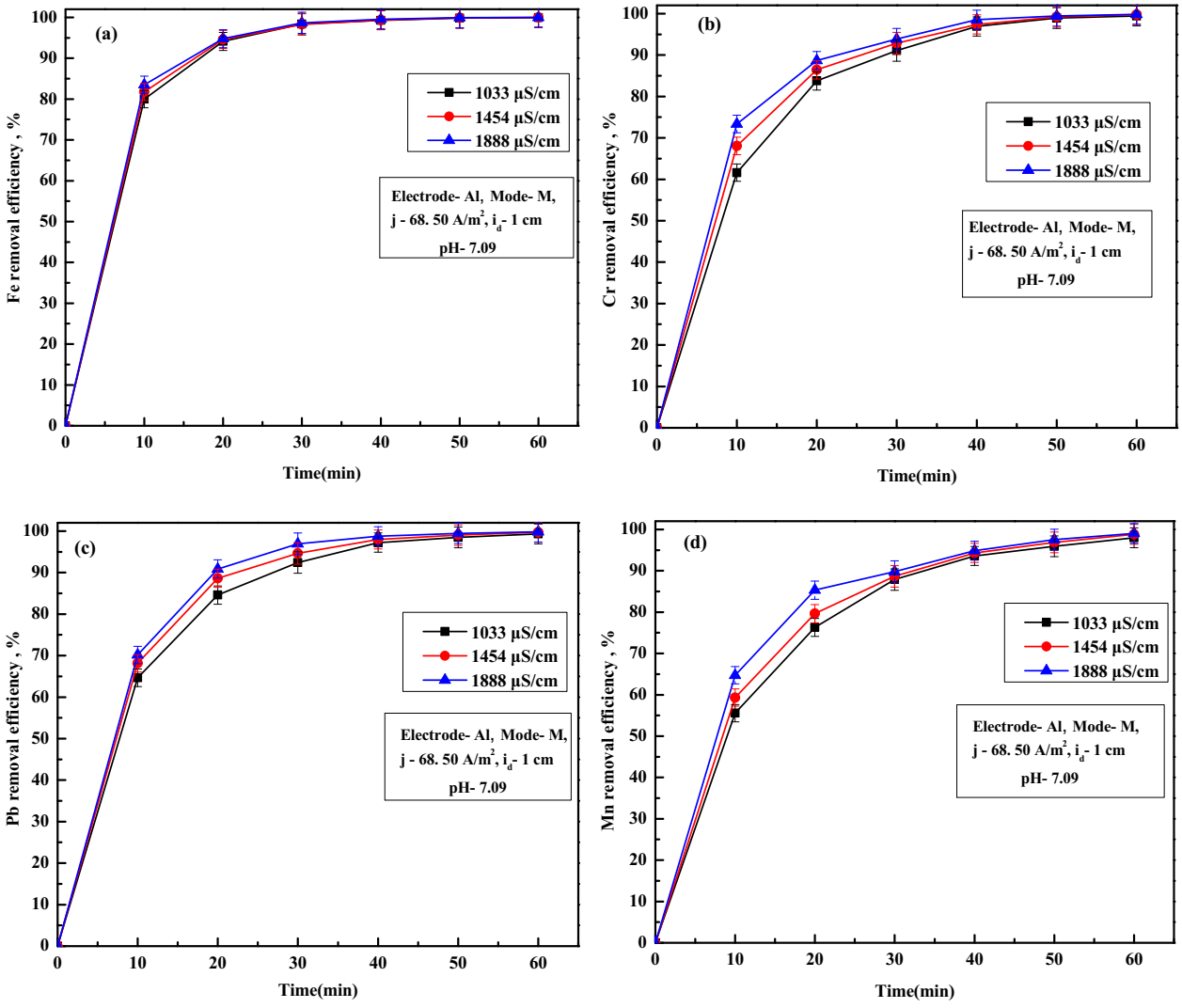

Fig. 8 Effect of solution conductivity on removal of (a) Fe, (b) Cr, (c) Pb and (d) Mn ions.

Table 8 Values of TDS, turbidity, salinity, conductivity, Al ions and Cu ions for different solution conductivity after 60 min of EC.

Initial conductivity (μS/cm)	TDS (mg/L)	Turbidity (NTU)	Salinity (mg/L)	Conductivity (μS/cm)	Al ions (mg/L)	Cu ions (mg/L)	EEC (kWh/m^3)
1033	85.45	0.89	92.61	522	0.72	0.07	3.93
1454	78	0.84	94.35	532	0.74	0.02	2.86
1888	72	0.79	97.25	547	0.75	0.01	2.4

Table 9 List of various metallic phases identified by XRD analysis and their JCPDS names and codes corresponding to different peaks (1–34) as shown in Fig. 9.

Sl. No	Reference Code	PDF index name	Chemical formula	Sl No	Reference Code	PDF index name	Chemical formula
1	PDF-00-038-1027	Aluminum Manganese	$Al_{86}Mn_{14}$	18	PDF-00-008-0269	Magnesium Zinc	Zn_3Mg_7
2	PDF-00-043-1154	Aluminum Titanium Vanadium	$Al_3Ti_{0.8}V_{0.2}$	19	PDF-00-044-1288	Titanium	Ti
3	PDF-01-072-2074	Calcium Nickel Silicon	$CaNi_{0.5}Si_{1.5}$	20	PDF-00-021-0759	Aluminum Copper Neodymium	AlCuNd
4	PDF-01-072-2046	Calcium Nickel Silicon	$CaNi_2Si_2$	21	PDF-00-034-0400	Aluminum Iron Samarium	Al_7Fe_5Sm
5	PDF-00-013-0450	Calcium Magnesium	$CaMg_2$	22	PDF-00-040-1111	Aluminum Manganese Silicide	$Al_{85}Mn_{14}Si$
6	PDF-00-033-0402	Chromium Phosphide	$Cr_{12}P_7$	23	PDF-00-020-0072	Aluminum Yttrium	Y_3Al
7	PDF-00-044-1088	Iron Nickel	$Fe_{0.96}Ni_{0.056}$	24	PDF-01-072-1027	Cerium Nickel Silicon	$Ce_3Si_2Ni_8$
8	PDF-00-003-0987	Copper Magnesium	Cu_2Mg	25	PDF-00-047-1012	Chromium Cobalt Iron Vanadium	$Co_{15}Cr_{23}$ Fe_{57} V_5
9	PDF-00-018-0459	Copper Titanium	Ti_2Cu_3	26	PDF-00-030-0456	Cobalt Samarium	Co_2Sm
10	PDF-00-029-0523	Cobalt Zinc	$CoZn_{13}$	27	PDF-00-037-1037	Copper Neodymium	$NdCu_4$
11	PDF-00-033-1017	Iron Nickel	FeNi	28	PDF-00-035-1093	Galium Manganese	GaMn
12	PDF-00-002-1267	Iron Silicon	FeSi	29	PDF-00-027-0223	Galium	Ga
13	PDF-00-034-0529	Iron	Fe	30	PDF-00-043-1379	Galium Magnesium	Ga_5Mg_2
14	PDF-01-071-0615	Magnesium Copper Phosphide	MgCuP	31	PDF-00-015-0096	Iron Yttrium	Fe_2Y
15	PDF-00-019-0797	Manganese Vanadium	MnV	32	PDF-00-018-0784	Magnesium Yttrium	MgY
16	PDF-00-001-1141	Manganese	Mn	33	PDF-01-081-1377	Neodymium Silicon	$NdSi_{1.25}$
17	PDF-00-035-0773	Magnesium Silicon	Mg_2Si	34	PDF-01-073-0117	Yttrium Cobalt	YCo

0.01 mg/L, residual conductivity risen from 522 to 547 μS/cm, salinity increased from 92.61 to 97.25 mg/L, and Al ions increased from 0.72 to 0.75 mg/L with the increase in conductivity from 1033 to 1888 μS/cm. Higher values of residual conductivity, salinity and Al ions were due to use of additional NaCl addition and higher amounts of $Al(OH)_3$ flocs generation. Considering the presence of higher amount residual Al ions as well as higher conductivity and salinity, lower solution conductivity of 1033 μS/cm was used for all the further experiments.

3.7. Characterization of EC generated sludge

Apart from Fe, Cr, Pb, Mn, Cu, Al ions, mineral beneficiation process water may contain many metal ions in traces. So, it was necessary to identify the removal of various other metal

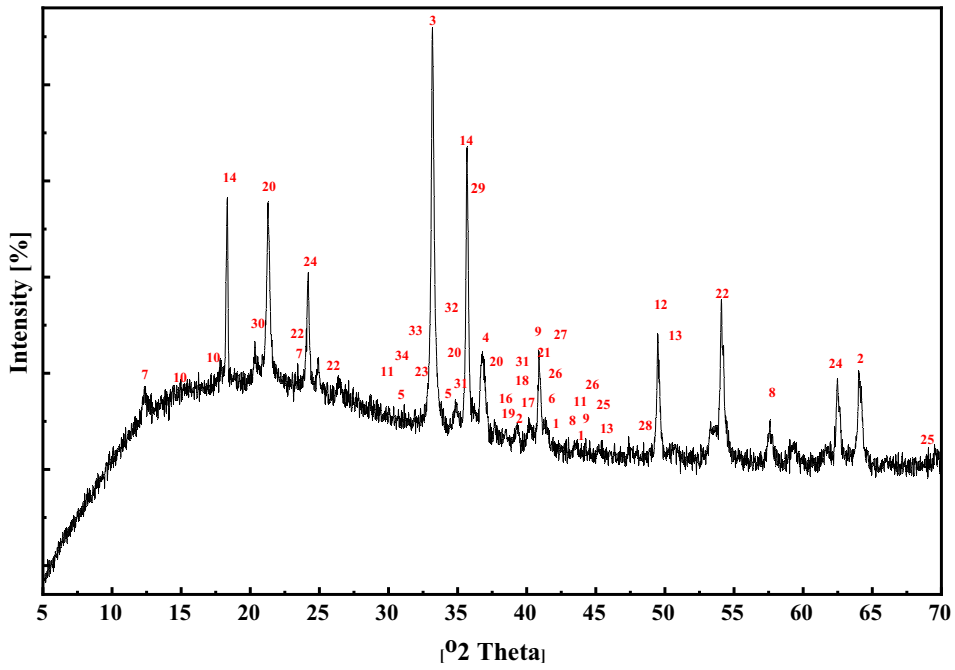

Fig. 9 X-ray diffraction patterns of the sludge generated after EC treatment.

Table 10 Comparison of the present work with reported work in literature for treatment of various mine and similar wastewater by EC.

Type of Wastewater	Water volume (mL), electrode and electrode area (cm^2)	CD (mA/cm^2) & EC Time (min)	Ion removal (%)	Reference
Sulphide Mineral processing wastewater	200, Al, 33	90.91, 120	93.14% SO_4^{2-}, 94.86% Ca^{2+}	Wu et al. (2019)
Mine water	500, Al/SS, 35	70, 120	74.7% Fe, 99% Cu, 99% Si, 40% Zn, 21.26% Mn, 28.9% SO_4	Nariyan et al. (2017)
Iron-rich acid mine drainage	250, Fe, 26.25	500, 60	99.9% Fe	Foudhaili et al. (2019)
Mine drainage	750, Fe, 24.2	20, 45	52% SO_4	Foudhaili et al. (2020a)
Antimony mine wastewater	500, Al, 18	16.66, 60	96% Sb	Zhu et al. (2011)
Gold mine wastewater	1500, Fe	20, 30	SO_4 (> 7.5%)	Foudhaili et al. (2020b)
Iron ore Beneficiation plant process water	3000, Al, 14.6	6.86, 60	99.95% Fe, 97.77% Cr, 99.34% 88.69% Pb, Mn, 73.44% Cu	Present work

ions present in water at a very lower quantity by EC. For this purpose, EC generated sludge was collected, dried and further XRD analysis was carried out to identify the presence of various metallic phases and results are shown in Fig. SM-4. All the XRD peaks present in the spectrum were matched with the JCPDS (Joint Committee on Powder Diffraction Standards) (JCPDS 1997) database file and results are summarized in Table 9. It can be observed from Fig. 9 that many metallic compounds of aluminum, iron, nickel, magnesium, cobalt, zinc, calcium, chromium, copper, manganese and silicide are present with higher intensities. Also, many low-intensity peaks corresponding to various other metals like titanium, samarium, galium, yttrium, etc. were also identified as observed from Table 9. Presence of all such metallic phases in sludge confirmed the removal of major metal ions like Fe, Cr, Pb, Mn and Cu along with other ions with trace concentrations such as nickel, cobalt, magnesium, titanium, vanadium, phosphide, zinc, neodymium, samarium, yttrium, etc. from process water. Such observations indicate that $Al(OH)_3$ coagulant formed during EC entraps most of the impurities and ions present in the process water.

3.8. Comparison of the present study with reported work

Comparison of the present work with similar reported work in literature using EC is shown in Table 10. From Table 10 it is noticed that, CD in the present study is lower than other works reported by investigators. Detailed analysis of literature infers

that EC treatment time to achieve sufficient removal in some studies (Wu et al., 2019; Nariyan et al., 2017) is higher compared to the present study. Also the working volume used by several authors are lower, it seems that excess energy was used in previous studies. From this point of view it is evident that the any EC studies needs to conduct with larger volume of water to make the process economical.

4. Conclusions

In the present study, process water collected from iron ore beneficiation plant was treated by electrocoagulation (EC) to obtain treated water suitable for reuse or safe for discharge as per WHO guidelines. Various metal ions present in water such as various metal ions such as Fe, Cr, Cu, Zn, Mn, Pb, Al and other pollutants like: TDS, turbidity, conductivity, and salinity were estimated before and after EC treatment to identify the influence of EC parameters on pollutant removal. Characterization of process water showed that water having 115.24 mg/L of Fe, 7.10 mg/ L of Cr, 2.68 mg/L of Pb, 0.96 mg/L of Mn ions as major along with 977 NTU turbidity. Residual Cu ions, Al ions, TDS, conductivity, salinity were found in WHO permissible limits. Based on the experimental results, it was observed that, aluminum electrodes at monopolar mode with current density of 68.50 A/m^2, inter-electrode distance of 1 cm and solution conductivity of 1.033mS are the ideal operating conditions to get treated water with removal efficiency of 99.95%, 99.46%, 99.33%, 97.99%, 73.44% for Fe, Cr, Pb, Mn and Cu ions respectively after 60 min of EC with electric energy consumption of 3.93 kWh/m^3 and operating cost of 0.6115 US$/$m^3$. It was observed that, with increase in current density from 34.25 to 86.20 A/m^2, residual Fe ion concentration decreases from 0.35 to 0.03 mg/L, Cr ion concentration decreases from 0.32 to 0.02 mg/L, Pb ion concentration decreases from 0.06 to 0.01 mg/L, Mn ion concentration decreases from 0.20 to 0.01 mg/L. Values of TDS, conductivity, salinity and pH of treated water were also found to be in WHO permissible the range. Kinetic analysis showed that metal ions removal followed the apparent first-order model. Characterization of EC generated sludge confirmed the removal of major elements like Fe, Cr, Cu, Zn, Mn, Pb, Al as well as trace elements such as Ni, Co, Mg, Ti, V, Zn, Nd, Sm, Y etc. from process water. Overall experimental results indicate that EC process could be used to treat iron ore beneficiation plant process water to make it suitable for reuse or safe for discharge.

Declaration of Competing Interest

The authors declare that they have no known competing financial interests or personal relationships that could have appeared to influence the work reported in this paper.

References

Akbal, F., Camcı, S., 2011. Copper, chromium and nickel removal from metal plating wastewater by electrocoagulation. Desalination 269, 214–222.

Al-Qodah, Z., Al-Qodah, Y., Assirey, E., 2020a. Combined biological wastewater treatment with electrocoagulation as a post-polishing process: A review. Sep. Sci. Technol. 55, 2334–2352.

Al-Qodah, Z., Al-Qudah, Y., Omar, W., 2019. On the performance of electrocoagulation-assisted biological treatment processes: a review on the state of the art. Environ. Sci. Pollut. Res. 26, 28689–28713.

Al-Qodah, Z., Al-shannag, M., 2017. Heavy metal ions removal from wastewater using electrocoagulation processes: a comprehensive review. Sep. Sci. Technol. 52, 2649–2676.

Al-Qodah, Z., Tawalbeh, M., Al-Shannag, M., Al-Anber, Z., Bani-Melhem, K., 2020b. Combined electrocoagulation processes as a novel approach for enhanced pollutants removal: A state-of-the-art review. Sci. Total Environ. 744, 140806.

Arefieva, O., Nazarkina, A.V., Gruschakova, N.V., Skurikhina, J.E., Kolycheva, V.B., 2019. Impact of mine waters on chemical composition of soil in the Partizansk Coal Basin, Russia. Int. Soil Water Conserv. Res. 7, 57–63.

Brooks, S.J., Escudero-Onate, C., Lillicrap, A.D., 2019. An ecotoxicological assessment of mine tailings from three Norwegian mines. Chemosphere 233, 818–827.

Canizares, P., Jimenez, C., Martınez, F., Saez, C., Rodrigo, M.A., 2007. Study of the electrocoagulation process using aluminum and iron electrodes. Ind. Eng. Chem. Res. 46, 6189–6195.

Das, D., Nandi, B.K., 2019a. Arsenic removal from tap water by electrocoagulation: Investigation of process parameters, kinetic analysis and operating cost. J. Disp. Sci. Technol. https://doi.org/10.1080/01932691.2019.1681280.

Das, D., Nandi, B.K., 2020. Removal of hexavalent chromium from wastewater by Electrocoagulation (EC): Parametric evaluation, kinetic study and operating cost. Trans. Ind. Inst. Met. 73, 2053–2060.

Das, D., Nandi, B.K., 2019b. Removal of Fe(II) ions from drinking water using Electrocoagulation process: Parametric optimization and kinetic study. J. Environ. Chem. Engin. 7, 103116.

Dhadge, V.L., Medhi, C.R., Changmai, M., Purkait, M.K., 2018. House hold unit for the treatment of fluoride, iron, arsenic and microorganism contaminated drinking water. Chemosphere 199, 728–736.

Elazzouzi, M., Haboubi, K., Elyoubi, M.S., 2019. Enhancement of electrocoagulation-flotation process for urban wastewater treatment using Al and Fe electrodes: Techno-economic study. Mater. Today: Proc. 13, 549–555.

Elnakar, H., Buchanan, I., 2020. Treatment of Bypass Wastewater Using Novel Integrated Potassium Ferrate(VI) and Iron Electrocoagulation System. J. Environ. Eng. (United States) 146, 1–8.

Foudhaili, T., Jaidi, R., Neculita, C.M., Rosa, E., Triffault-Bouchet, G., Veilleux, É., Coudert, L., Lefebvre, O., 2020a. Effect of the electrocoagulation process on the toxicity of gold mine effluents: A comparative assessment of Daphnia magna and Daphnia pulex. Sci. Total Environ. 708, 134739.

Foudhaili, T., Lefebvre, O., Coudert, L., Neculita, C.M., 2020b. Sulfate removal from mine drainage by electrocoagulation as a stand-alone treatment or polishing step. Miner. Eng. 152, 106337.

Foudhaili, T., Rakotonimaro, T.V., Neculita, C.M., Coudert, L., Lefebvre, O., 2019. Comparative efficiency of microbial fuel cells and electrocoagulation for the treatment of iron-rich acid mine drainage. J. Environ. Chem. Eng. 2019, 103149.

Govindan, K., Sumanasekara, V.D.W., Jang, A., 2020. Mechanisms for degradation and transformation of β-blocker atenolol: Via electrocoagulation, electro-Fenton, and electro-Fenton-like processes. Environ. Sci. Water Res. Technol. 6, 1465–1481.

Hashim, K.S., Shaw, A., Al Khaddar, R., Ortoneda Pedrola, M., Phipps, D., 2017. Defluoridation of drinking water using a new flow column-electrocoagulation reactor (FCER) – Experimental, statistical, and economic approach. J. Environ. Manage. 197, 80–88.

Lu, J., Wang, Z.R., Liu, Y.L., Tang, Q., 2016. Removal of Cr ions from aqueous solution using batch electrocoagulation: Cr removal mechanism and utilization rate of in situ generated metal ions. Process Saf. Environm. Protec. 104, 436–443.

Modirshahla, N., Behnajady, M.A., Aghdam, S.M., 2008. Investigation of the effect of different electrodes and their connections on the removal efficiency of 4-nitrophenol from aqueous solution by electrocoagulation. J. Haz. Mat. 154, 778–786.

Naidu, G., Ryu, S., Thiruvenkatachari, R., Choi, Y., Jeong, S., Vigneswaran, S., 2019. A critical review on remediation, reuse, and resource recovery from acid mine drainage. Environ. Poll. 247, 1110–1124.

Nariyan, E., Sillanpää, M., Wolkersdorfer, C., 2017. Electrocoagulation treatment of mine water from the deepest working European metal mine – Performance, isotherm and kinetic studies. Sep. Purif. Technol. 177, 363–373.

Qina, W., Hana, D., Songa, X., Engesgaard, P., 2019. Effects of an abandoned Pb-Zn mine on a karstic groundwater reservoir. J. Geochem. Explor. 200, 221–233.

Shahedi, A., Darban, A.K., Taghipour, F., Jamshidi-Zanjani, A., 2020. A review on industrial wastewater treatment via electrocoagulation processes. Curr. Opin. Electrochem. 22, 154–169.

Silva, A.M., Cunha, E.C., Silva, F.D.R., Leão, V.A., 2012. Treatment of high-manganese mine water with limestone and sodium carbonate. J. Cleaner Prod. 29–30, 11–19.

Silva, J.F.A., Graca, N.S., Rebeiro, A.M., Rodrigues, A.E., 2018. Electrocoagulation Process for the removal of co-existent fluoride, arsenic and iron from contaminated drinking water. Sep. Purif. Technol. 197, 237–243.

WHO, 2004. Guidelines for Drinking Water Quality, Recommendations. World Health Organization, Geneva.

Wu, M., Hu, Y., Liu, R., Lin, S., Sun, W., Lu, H., 2019. Electrocoagulation method for treatment and reuse of sulphide mineral processing wastewater: Characterization and kinetics. Sci. Total Environ. 696, 134063.

Zhu, J., Wu, F., Pan, X., Guo, J., Wen, D., 2011. Removal of antimony from antimony mine flotation wastewater by electrocoagulation with aluminum electrodes. J. Environ. Sci. 23, 1066–1071.